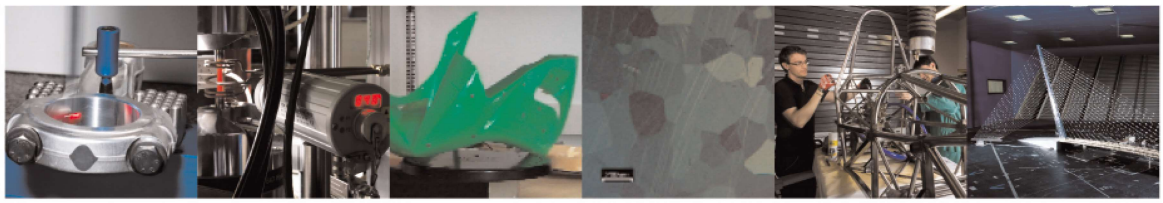

Layer-wise control of selective laser melting by means of inline melt pool area measurements

Vasileska, Ema; Demir, Ali Gökhan; Colosimo, Bianca Maria; Previtali, Barbara

LAYER-WISE CONTROL OF SELECTIVE LASER MELTING BY MEANS OF INLINE MELT POOL AREA MEASUREMENTS

Ema Vasileska, Ali Gökhan Demir, Bianca Maria Colosimo, Barbara Previtali

Department of Mechanical Engineering, Politecnico di Milano, Via La Masa 1, 20156 Milan, Italy

Abstract

Industrial selective laser melting systems commonly employ a fixed set of process parameters throughout the build of the same component. The process parameters are commonly set by experimental studies carried out on simple geometries to achieve high density. A common issue is related to the fact that the single set of parameters can be inadequate for small sections and overhang regions, where thermal accumulation can occur. An online adaptation of process parameters is required for avoiding such issues and defects that commonly arise such as the swelling phenomenon. A real-time control strategy would be desirable. However, the real time control requires fast acquisition and reaction in the order of microseconds. Another approach is to provide corrective actions in a layer-wise fashion by elaborating the monitoring data collected during the previous layer. Therefore, this work proposes a layer-wise control strategy based on coaxial melt pool monitoring. To this purpose, an open SLM platform is employed, fitted with a CMOS camera viewing the process emission in near infrared region. Initially, the acceptable level of the melt pool area is defined on a simple geometry. Then, the melt pool area is monitored on more complex shapes. The melt pool area measured on each vector of a given layer is used to compensate the energy density of the same vector at the next layer. The results show an effective reduction of swelling defects on small geometries with fine details.

Key words: SLM, coaxial process monitoring, melt pool monitoring, pulse width modulation, process control

Introduction

Selective laser melting (SLM) is a metal additive manufacturing process that is achieving extensive industrial acceptance. Among the others, benefits provided are the possibility for manufacturing complex geometries, lightweight structures, and internal channels, improving the product performance, which otherwise would be impossible with traditional manufacturing processes. SLM also provides means for producing high value products in small lots, which require defect-free manufacturing. Nevertheless, for a wider acceptance of SLM techniques in highly regulated industrial fields, such as aerospace or medical sectors, consistent quality and long-term performance of additively manufactured metallic parts are required to satisfy industrial standards and marketing needs [1,2,3].

Most commonly, both in industrial and research environment, the same set of parameters is employed throughout the scanning of the whole workpiece. This set of scanning parameters is experimentally proven to result in a high-density fabrication of the part, and is found by a number of trial-and-error testings which lead to a large consumption of raw material, energy input and time. However, this parameter set does not consider the part geometry or any potential in-process defects. The part geometry has a large impact on the melting conditions and the final quality of the workpiece. Examples for critical features in the geometry, which result in poor surface roughness, are overhangs and acute corners [4]. In order to maintain the quality of the final workpiece, it is essential to implement process monitoring together with a feedback control of the scanning parameters which are regulated depending on the process output behaviour.

Offline simulations of the melting process (FEM) combined with machine learning are giving the opportunity for open-loop optimisation of process parameters, which theoretically achieve desired final properties [4,5]. However, efficient simulation tools able to adapt process parameters depending on part geometry are still to be developed. Implementing an effective closed-loop control solution with sensor feedback is still in research phase for SLM technology. There are significant barriers for adoption of real-time control in SLM; such as high sampling rates required to capture the fast solidification dynamics of the material, as well as lack of appropriate models for online estimation and control [7,8]. According to Fox et al. [9] it is sufficient to control melt pool dimensions throughout the entire process in order to ensure robust product qualities. Among the melt pool feedback controllers found in the literature, most target the melt pool area. A real-time feedback control has been employed by Kruth et al. [10] and Craeghs et al. [11] on overhang structures and cubes, using a photodiode and CMOS camera for measuring the melt pool indicators and varying the laser power based on the sensor signal. Yeung et al. [12] implemented a high-speed coaxial camera on an SLM platform and presented a jerk-limited motion control for improving the position and

velocity accuracy, as well as a thermal-adjusted strategy which locally varies laser power based on adjacent solidified material. Renken et al. [13] closed the loop in real time with a pyrometer implemented in an FPGA environment and achieved reduction of the deviation of process temperature which led to more stable conditions in the melt pool. Throughout the research works, it is confirmed the potentiality of improving the quality and microstructure of the SLM fabricated part with adapting the process parameters by continuously observing the thermal behaviour of the melting process [14]. Indeed, several machine manufacturers have started implementing coaxial monitoring equipment in order to monitor the melt pool conditions. However, effective control strategies exploiting these sensors are yet to be developed [15]–[18].

Therefore, this work proposes a novel control scheme based on coaxial monitoring and correction of energy density of each scanned vector of the next layer. In the initial part of the work the layer-wise control concept is introduced along with candidate control strategies. Later, an experimental campaign is presented to build an empirical model linking duty cycle and scan vector length to melt pool area. Next, the use of the candidate control strategies is simulated on different geometries by estimating the melt pool area behaviour with the empirical model. Finally, the most advantageous control method is validated by experimental runs.

Layer-wise control concept

In SLM, the implementation of real time control can be cumbersome due to temporal and dimensional scale of the physical phenomenon involved. Accordingly, a layer-wise control strategy can be employed to correct or limit the propagation of the process defect among the successive layers. Swelling is one of the SLM defects, which is defined as deposited material extruding from the powder bed, due to excessive thermal accumulation. Resultantly, the geometrical accuracy is comprised. These regions can wear the powder recoater or eventually be stripped off by the recoater. Pointy edges, thin sections, overhang regions or poorly supported sections are more prone to heat accumulation and hot spot formation, where swelling phenomenon can be more critical [19].

The energy input can be managed in order to avoid the swelling phenomenon. The laser energy density E is a common parameter used to define the energy delivered at unit volume material and is defined as:

$$E = \frac{P_{peak} \cdot \delta}{h \cdot z \cdot v} \qquad (1)$$

where h is the hatch distance, z is the layer thickness, v is the scanning speed, P_{peak} is the peak laser power, and δ is the duty cycle. For systems operating at continuous wave (CW) emission the duty cycle δ equals to 1, while the systems operating with pulsed wave (PW) emission by power modulation the duty cycle varies [20]. For a given material these process parameters are commonly set to achieve high density (i.e. >99%) on simple geometries such as cubical samples, and variations according to the part geometry is usually not considered. Therefore, the adaptability of the same process parameters to both bulky parts and fine structures is limited. Assigning different process parameters to different parts, as well as different sections of the same part is possible to most of the industrial SLM systems (see Fig. *1*). Varying process parameters within the layer in order to avoid heat accumulation is a promising concept that requires further studies.

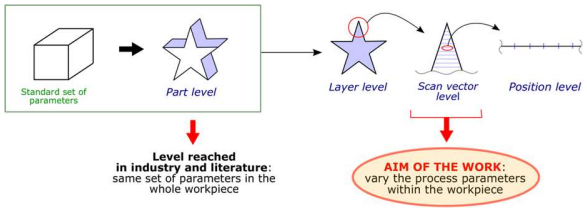

Fig. 1. Variation of process parameters at different levels.

From this point of view, controlling the energy density by modulating the laser power at the heat accumulation zones, and hence the swelling regions, is the core of the layer-wise control strategies. Fig. *2* shows a schematic representation of the proposed control strategy. In order to reveal the heat accumulation zones, coaxial monitoring of the melt pool via a CMOS camera is the chosen method. The reference melt pool size is determined through the common practice of producing samples with simple shapes such as cubes with process parameters determining the desired density. The control method aims to adjust the duty cycle in order to maintain the melt pool size at the correct value.

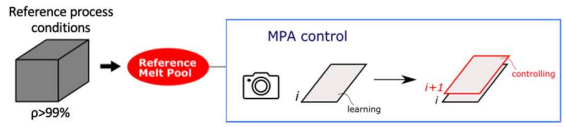

Fig. 2. Schematic representation of the layer-wise control strategy.

In the layer-wise control concept, the scanning process of the preceding layer is evaluated in order to correct the melting condition in the following layer at the points where it deviates from the desired behaviour. For analysing the correctness of the scanning process, the melt pool area (*MPA*) is considered as a of the thermal behaviour during the process. By monitoring the melt pool, the amount of laser energy delivered to the part can be indirectly observed. If an excess or a lack of energy input is observed, the scanning parameters need to be modified in order to stabilize the process.

The layer-wise control strategy works such that it calculates and evaluates the average melt pool area of the scan vector k in the layer i, and corrects the delivered energy density in the same scan vector k in the subsequent layer $i+1$, by adjusting the duty cycle of the laser power. In the case when the melting process of a scan vector in the previous layer is optimal, then the equivalent duty cycle will be employed likewise in the following layer. In this way, the faulty melting conditions are instantaneously corrected and the defect propagation in the height of the build is avoided.

Candidate strategies for layer-wise control

Amongst several possibilities, two different approaches were examined for the layer-wise control, with *fixed* and with *adaptive* reference point. In both methods, the melt pool area was employed as a process variable, and the duty cycle of the laser power as a process parameter. The error of the melt pool area of the scan vector k in layer i ($e_{k,i}$), is computed as the difference between the nominal melt pool area MPA_{nom} and the melt pool area $(MPA_{k,i})$ acquired when scanning the same scan vector k and layer i. Depending on the value of the error, a negative sign indicates under-heated melting process, while a positive error indicates an over-melting phenomenon.

$$e_{k,i} = MPA_{nom} - MPA_{k,i} \qquad (2)$$

The difference between the two approaches for layer-wise control is the method for calculating the corrected duty cycle $\delta_{k,i+1}$ as a function of the error of the melt pool area $e_{k,i}$ and the duty cycle employed in the previous layer $\delta_{k,i}$ for the corresponding scan vector k. The control schemes of the layer-wise control strategies are shown on Fig. *3* and Fig. *4* respectively, where *MPA* is the melt pool area of the melt pool *MP* acquired with the camera and obtained from the image analyses algorithm, and d are the disturbances in the process which can be a result of the process itself, or of the powder material, gas flow, or the recoating system.

When the layer-wise control with *fixed* reference point is considered, the adjusted duty cycle $\delta_{k,i+1}$ is found as a sum of the previous duty cycle $\delta_{k,i}$ and a correction factor $\Delta\delta_{k,i+1}$. The correction factor $\Delta\delta_{k,i+1}$ is computed as a function of the error of the melt pool area $e_{k,i}$.

$$\delta_{k,i+1} = \delta_{k,i} + \Delta\delta_{k,i+1}(e_{k,i}) \qquad (3)$$

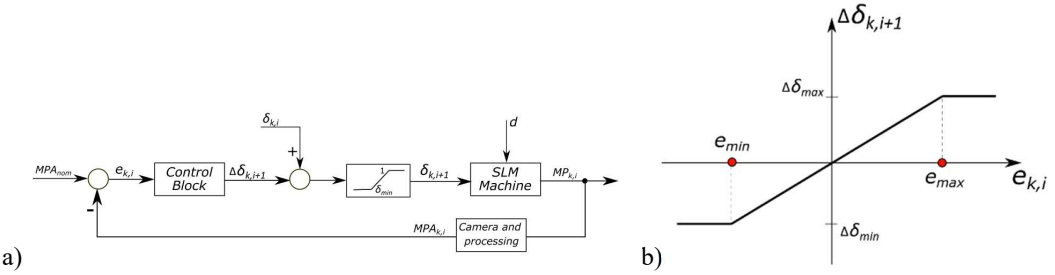

a) b)

Fig. 3. Layer-wise control with fixed reference point: a) Control scheme b) Control graph.

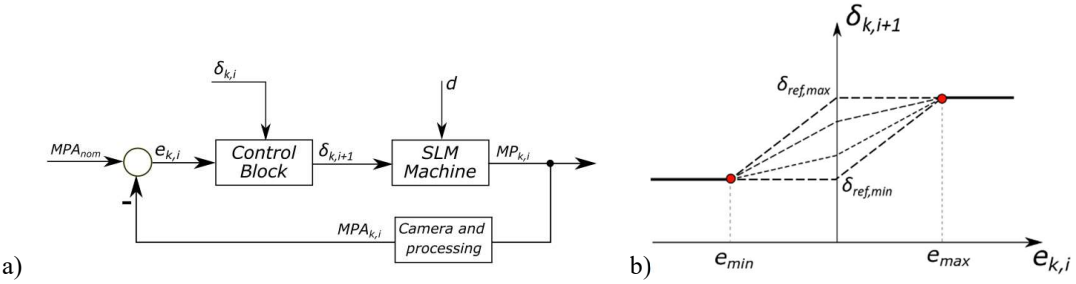

Fig. 4: Layer-wise control with adaptive reference point: a) Control scheme b) Control graph with variable reference point.

In the control strategy with *adaptive* reference point, the reference point of the duty cycle is modified between $\delta_{ref,max}$ and $\delta_{ref,min}$ in the control graph (Fig4.b) at each scan vector of every layer. For a given layer and scan vector, the duty cycle of the previous layer is taken as the reference point ($\delta_{k,i}= \delta_{ref,k,i+1}$). Then, the control graph is adjusted to constitute two linear relationships in the negative and positive *MPA* error regions. The duty cycle is calculated using these adapted relationships for $e_{k,i}$. The control graph is therefore adapted for each vector and layer.

Experimental inputs and strategy choice

Both the control strategies require experimental inputs. The reference melt pool area is determined by printing a simple bulk geometry scanned with nominal process parameters. The experimental model is derived to define the maximum (e_{max}) and minimum (e_{min}) error levels as well as the duty cycle levels. A straightforward approach to investigate the thermal accumulation behaviour is to vary the scan length (l_{sv}) at each scanned layer with the use of a triangle geometry. Shorter vectors are more prone to thermal accumulation due to the reduced duration between consecutive vectors. Hence, the experimental campaign was designed to evaluate the influence of the duty cycle and the scan length on the melt pool area. The measured data were used to fit the empirical model linking melt pool area (response) as a function of the duty cycle and the scan length. This transfer function was then used for experimental validation.

Experimental setup

Open Selective Laser Melting platform

An open and custom-made SLM platform namely *Penelope* was used to conduct the experimental work. The system is characterized by a working volume of 60x60x20 mm^3 and the ability to process small amount of powder. The powder bed is placed in a closed chamber where an inert atmosphere is created. The laser source employed in the experiment is a single mode fiber laser (IPG Photonics YLR-150/750-QCW-AC, Cambridge, MA, USA) with maximum power of 250 W and it can emit in continuous wave (CW) and can be modulated to emit at pulsed wave (PW) regime with maximum modulation frequency of 10 kHz. The laser optical chain consists of a collimating unit with focal length of 50 mm, a focus shifting two-lens system (VarioScan 20, Scanlab, Puchheim, Germany) and a 420 mm f-theta lens, while the deflection of the laser beam towards the building platform is achieved using two galvanometric mirrors. The scanning parameters and trajectory are set using Scanmaster software (Cambridge Technologies, Bedford, MA), whereas the control of the movement of the mechanical system and the chamber pressure are employed in LabVIEW environment (National Instruments, Austin, TX). The main specifications of the open SLM platform and its optical chain can be found on Table 1.

Table 1. Main characteristics of the open SLM platform

Parameter	**Value**
Laser emission wavelength, λ	1070 nm
Max. laser power, P_{max}	250 W
Beam quality factor, M^2	1.1
Nominal beam diameter on focal plane, d_0	70 μm

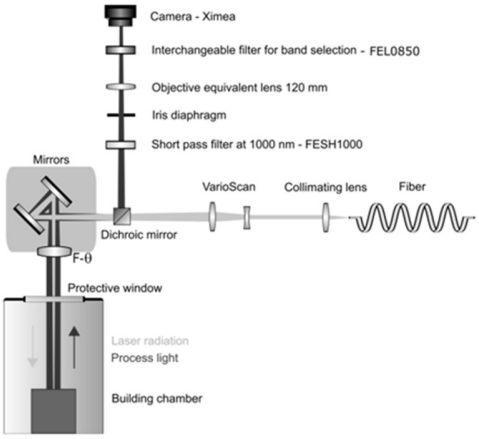

Fig. 5. Optical chain of the co-axial monitoring setup employed in the experiments

Material

Gas-atomized stainless steel AISI 316L (Cogne Acciai, Brescia, Italy) powder was used throughout the work. The powder packing density was 4.07 g/cm^3, while the powder size distribution was measured as D_{10}: 22.9 µm, D_{50}: 31.9 µm; D_{90}: 44.3 µm.

Monitoring module

The monitoring module was mounted between the scanner head and the focus variation optics (see Fig. *5*). The melting zone was coaxially viewed through a dichroic mirror reflective between 400 and 1000 nm. A 120 mm focusing lens (Camera Adapter, Scanlab GmbH, Puchheim, Germany) was used to fix the image plane with a focal length of 120 mm. As the laser beam scans the powder, the process emission is reflected back through the f-theta lens, the galvanometric mirrors and the dichroic mirror towards the camera sensor. Furthermore, implementing different optical filters along the path of the reflected process light can capture various desired emission bands. Thermal emission images between the range of 850 and 1000 nm were acquired by employing two optical filters in order to view only the near infrared (NIR) region (FELO850, and FSH1000, Thorlabs, Newton, NJ, USA). An industrial CMOS camera (Ximea xiQ USB Vision, Münster, Germany) was installed, with a sensor size of 1280 x 1204 pixel^2 and pixel size of 4.8 x 4.8 µm^2. By adapting the region of interest, the field of view was adjusted to 4.3 x 4.3 mm^2 with a spatial resolution of 14 µm/pixel, which permits an acquisition rate of 1200 fps.

The monitoring module provides a compromise between spatial and temporal resolution. With the given frame rate and a scan speed of 400 mm/s used in the experimental part of this work, the melt pool is observed at a distance of 332 µm between each frame. The total duration of capture, data transfer, data processing, and the reaction phases was calculated as approximately 1.4 ms. This duration exceeds the period between each frame (0.83 ms) and corresponds to a spatial displacement of 560 µm. Within the given conditions the use of a real time control system is not feasible. Hence the use of layer-wise control strategies become more advantageous.

Measurement of the melt pool area

After obtaining the NIR images, an image processing algorithm was used to measure the melt pool area. In the present work, the focus was put on the melt pool area as a key indicator for process stability.

The molten pool size is estimated performing static thresholding on thermal emission images of the molten pool, using an in-house developed MATLAB routine [21]. Thresholded images are binary matrices whose elements are 1 or 0 based on whether their original values were higher (or equal) or smaller than the threshold value. The threshold constant (C) was set matching the area measurements with an external illuminator and the area computed from the NIR images. The ejected particles and spatters were isolated from the main melt pool.

In the abovementioned image processing procedure, the melt pool area is defined as the sum of the pixels above a certain brightness level, without considering spatter ejection blobs, multiplied by the square of the spatial resolution. The melt pool area of frame number *k* can be calculated using the following equation:

$$MPA_k[mm^2] = r^2 \cdot \sum_{i=1}^{m} \sum_{j=1}^{n} {p^T}_{k_{i,j}} \qquad (4)$$

where *r* is the spatial resolution, $p_{k_{i,j}}$ is the gray level of the pixel in row i and column j of the frame k, and ${p^T}_{k_{i,j}}$ is the binary value of $p_{k_{i,j}}$ according to the threshold constant C, calculated as follows.

$${p^T}_{k_{i,j}} = \begin{cases} 1 & p_{k_{i,j}} \geq C \\ 0 & p_{k_{i,j}} < C \end{cases} \qquad (5)$$

The measured MPA at each frame was assigned to the spatial position on the scan plane by means of a normalized cross correlation algorithm. In the absence of the processing laser, the scan pattern was executed with the use of an external illuminator and the powder bed was observed with the coaxial monitoring module. The normalized cross correlation function was used on these images to calculate the relative displacement between frames. By iteratively employing this procedure on consecutive frames, a position map for each layer can be reconstructed [22].

Empirical model of the melt pool area as a function of scan length and duty cycle

Experimental design

A square geometry with 5 mm side was scanned in CW regime for the purpose of finding the nominal melt pool area that is signifying a stable melting process, as it was experimentally proven to result in a high density solid object with ρ > 99.5%. Melt pool videos were acquired throughout the build.

Table 2. Fixed and varied scanning parameters employed in the experiment

Fixed parameters	
Layer thickness [μm]	50
Hatch distance [μm]	70
Scan speed [mm/s]	400
Peak power [W]	200
Modulation frequency [kHz]	3
Scan direction [°]	0
Scan strategy	Serpentine
Varied parameters	
Duty cycle	0.3 - 1.0
Scan vector length [mm]	0.05 - 5.0

An equilateral triangle with 5 mm side was chosen as the test geometry in order to investigate how the scan vector length affects the melt pool area, since it is a simple shape with a continuously changing scan vector length. The effect of the amount of energy input on the melt pool is investigated by varying the duty cycles from 0.3 to 1. Each triangle was scanned starting from the longest scan vector and ending with the shortest scan vector at the edge of the triangle. The peak laser power was fixed to 200 W and the scanning velocity to 400 mm/s, while the hatch distance and layer thickness were 70 μm and 50 μm respectively. These process parameters are confirmed through preliminary experiments to successfully fabricate a part obtaining high density when the laser is scanning in CW regime. Thirty layers were executed without changing the scan direction between layers. Two replications were produced for all conditions. *Table 2* summarizes the fixed and varied set of parameters used in the experiment.

Melt pool analysis

The nominal melt pool area was determined at 0.46 mm^2 observing the monitoring images of the square shaped sample. Fig. 6 shows the melt pool area maps on the triangle specimens as a function of the duty cycle. It can be concluded

that the melt pool area is highly affected by the duty cycle, which, combined with the scan length, is basically determining the average laser power that is locally used. The duty cycles of 0.4 and 0.3 resulted in under-melting of the part throughout the whole scan, and the scan vector length had no influence on the melt pool area. When scanning with duty cycles higher than 0.4, there was an increasing trend of the melt pool area as the scan vector length decreased. Towards the end of each triangle an enlargement of the melt pool area was observed, as the scan vector was getting shorter and there was less time for heat dissipation, which resulted in larger overheating.

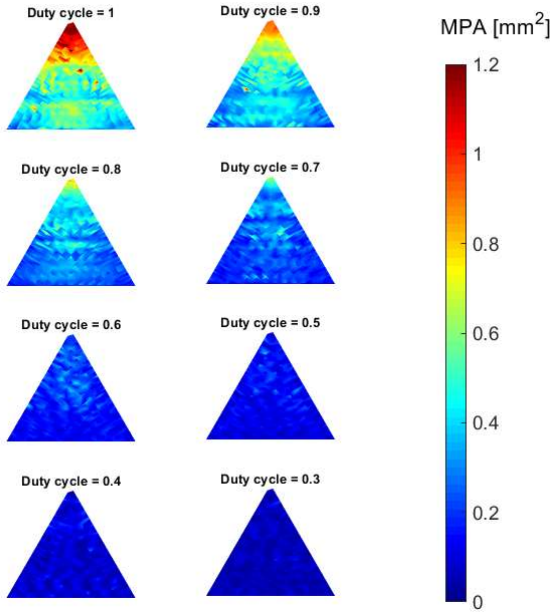

Fig. 6. Position-domain colour maps of melt pool area per duty cycle in triangular shaped workpiece, layer no 20.

The high values of melt pool area in the larger duty cycles occurred on the same position throughout the layers, thus creating a whole volume area where anomalous melt pools were detected. This indicated the occurrence of unwanted process phenomena during the building process, which influenced the building also in the following layers. In the areas where the over-melting phenomenon was present, swelling was eventually observed on the built specimens.

Developed empirical model

The monitoring images were analysed to calculate the average MPA for each scan vector length and duty cycle combination. Conditions corresponding to duty cycles lower than 0.5 were excluded from the analysis, since these conditions corresponded to undermelting without a significant change on the measured melt pool area. A regression model was fitted to the experimental data with the following mathematical expression.

$$\ln(MPA) = -3.0153 + 3.843 \cdot \delta - 0.2241 \cdot l_{sv} - 0.860 \cdot \delta^2 + 0.00912 \cdot {l_{sv}}^2 \qquad (6)$$

The model was found to fit the experimental data well with R_{adj}^2=98.61%, while normality and homogeneity of the residuals were verified. A comparison between the experimental data and the data fitted with the model is presented on Fig. *7*.

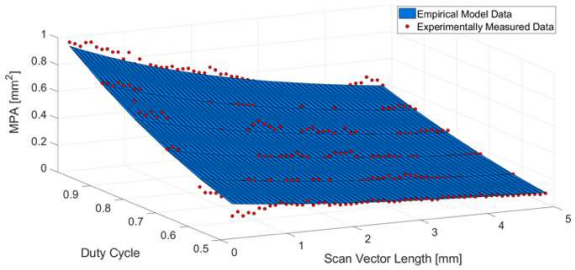

Fig. 7. Melt pool area as a function of scan vector length and duty cycle with a comparison between experimentally data and the fitted model.

Selection of the control strategy

Experimental constants

The data coming from the experimental runs were used to determine the experimental constants. It was observed that the duty cycles lower than 0.5 generated under-melting conditions, where the limit condition for e_{max}=0.30 mm^2. Over melting conditions were defined for e_{min}=-0.48 mm^2. The duty cycle was varied between δ_{min}=0.6 and δ_{max}=1.0 for the adaptive reference point. Analogously, the duty cycle was compensated in the fixed reference point with $\Delta\delta_{min}$=-0.4 and $\Delta\delta_{max}$=0.4.

Simulation of the control strategy responses

The empirical model was used to simulate the response of the proposed control strategies. The average melt pool area was calculated for two different geometries. Tests were done on two simple geometries with pointy edges prone to thermal accumulation. Fig. *8* shows the triangle and 4-point star chosen for the simulations. In the simulations, the first layer was scanned with two extreme duty cycles (1 and 0.6). The data of the melting process of the first layer, which is used by the control strategy to learn how to modify the laser power in the next layer, is real data acquired when the exact geometry with the specified duty cycle is scanned. Starting from the second layer, the scanning of the following layers was simulated with controlled parameters. Here, the laser power of each scan vector of the subsequent layer was adapted depending on the melt pool area generated by the empirical model at the same scan vector in the previous layer.

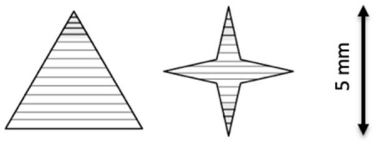

Fig. 8. Simulation geometries.

Fig. *9* compares the average melt pool area achieved by the two different control schemes as a function of layer number, starting duty cycle, and scanned geometry.

When the initial layer is scanned in CW mode (δ=1), the peaks of the workpieces start to overheat. After the control was employed, a small overshoot around the first layers was noticed in both control approaches, but ultimately they both stabilized the process and kept the melt pool area at its nominal value.

When the PW regime (δ=0.6) was adopted, the part was not sufficiently melted in the first layer before the control was applied, followed by a small overshoot of the melt pool area when the control tried to increase the duty cycle, before finally bringing and keeping the melt pool area on the steady-state value.

It was observed that the two schemes performed similarly, while the *fixed* reference point had a slightly faster response time compared to the control with *adaptive* reference point. Both strategies eventually stabilized the melting process. The control with fixed reference showed better results in terms of number of layers needed to bring the melt pool area

to the reference value for the star geometry, indicating a more suitable condition for different geometries. Moreover, the simpler control scheme of the fixed reference point was found to be more appropriate to reduce to computational burden. With this conclusion, the layer-wise control strategy with *fixed* reference point was chosen to be implemented.

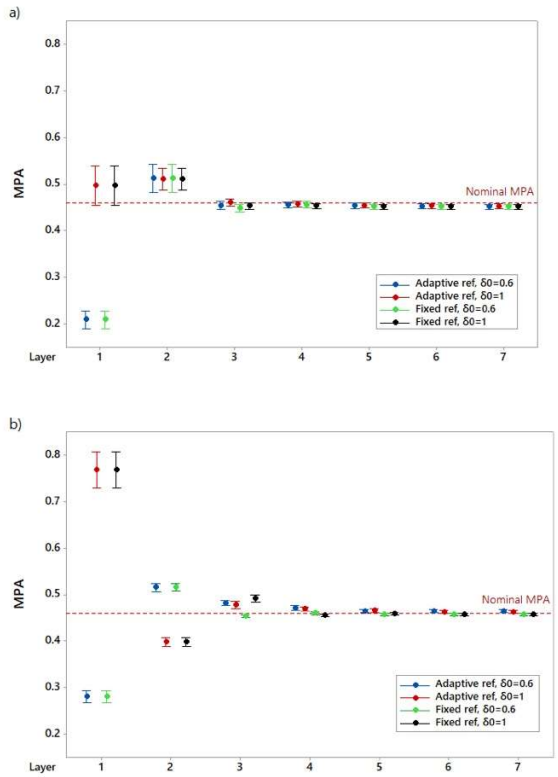

Fig. 9. Simulation and comparison of the time response of the two layer-wise correction strategies: a) triangle-shaped workpiece; b) star-shaped workpiece.

Validation of the control strategy

In order to validate the layer-wise control strategy, experiments were carried out on the 4-point star and the triangle shapes. Specimens without any control were also produced for comparison. Two replications were produced for both geometries, each one consisting of twenty-one layers. The melt pool area was monitored and computed throughout each layer, and this information was used to correct the successive layers with the *fixed* reference point control strategy. The duty cycle employed in the first layer was equal to 1 for the entire layer. 3D melt pool maps were produced based on the experiment output. Focus variation microscopy was used on the produced specimens for a 3D reconstruction of the sample surfaces. Mean standard error of surface geometry was calculated from the reconstructions. The process parameters for the validation tests are reported in Table 3.

Table 3. Fixed and varied parameters employed in the validation experiments

Fixed parameters	
Layer thickness [µm]	50
Hatch distance [µm]	70
Scan speed [mm/s]	400
Power [W]	200
Modulation frequency [kHz]	3
Scan direction [°]	0
Scan strategy	Serpentine
Initial duty cycle	1

Varied parameters	
Control strategy	None; Layer-wise

Fig. *10* and Fig. *11* show the melt pool maps for triangle and star shapes without and with the layer-wise control. It can be seen that without the process control the melt pool enlarges towards the pointy edges of the parts as the layer number progresses. The melt pool exceeds a value of 1 mm^2 around the overheated regions corresponding to the last scanned vectors in both geometries.

Implementing the layer-wise control, it can be seen that a more homogenous melt pool map can be obtained. It can be observed that the first layer of both the geometries show overheating regions. The use of the layer-wise control strategy successfully avoided the progression of the overheating regions along the successive layers. For both the geometries with the use of the layer-wise control strategy, the melt pool could be maintained within the chosen MPA error margins.

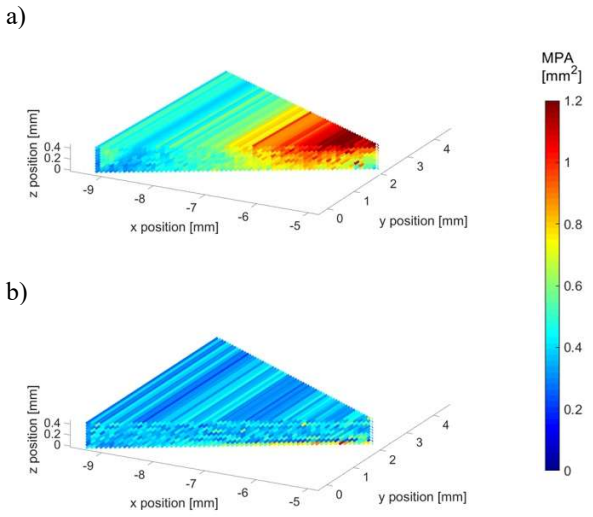

Fig. 10. Melt pool areas measured by the monitoring system during the production of the triangle shaped specimens a) without and b) with the layer-wise control.

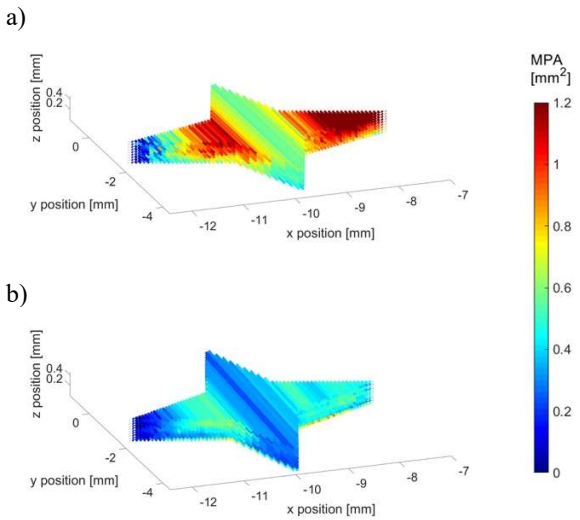

Fig. 11. Melt pool areas measured by the monitoring system during the production of the star shaped specimens a) without and b) with the layer-wise control.

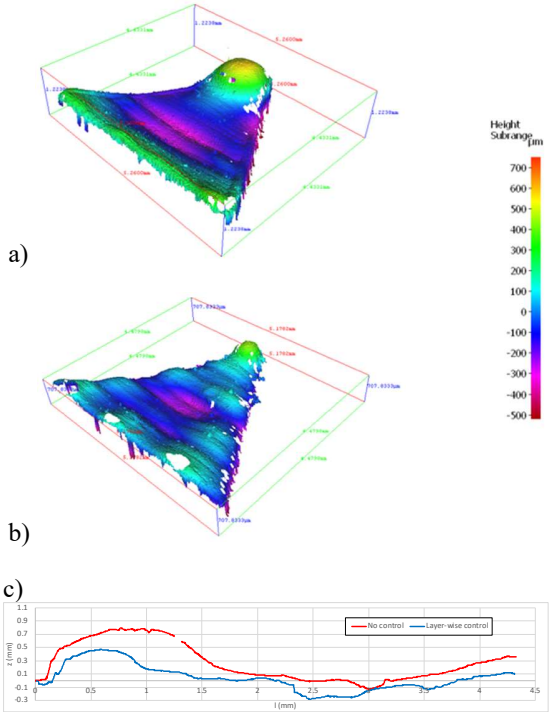

Fig. 12. 3D reconstructions of the produced triangle specimens a) without (MSE= 8.75 mm^2) and b) with layer-wise control (MSE= 1.54 mm^2). c) Height map from taken perpendicular to the scan direction along the centre.

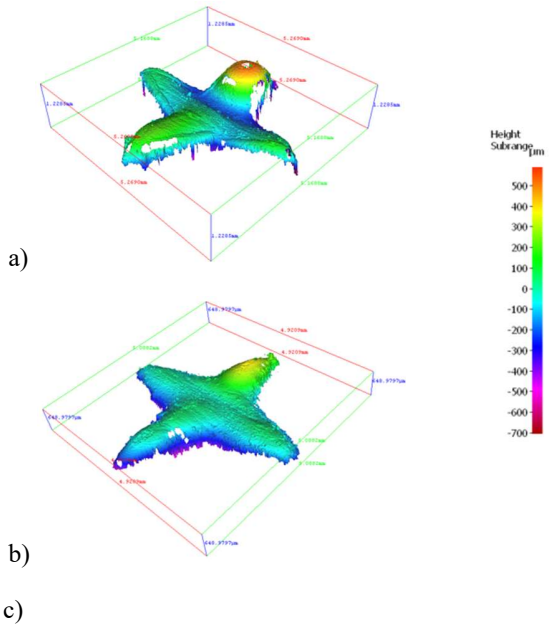

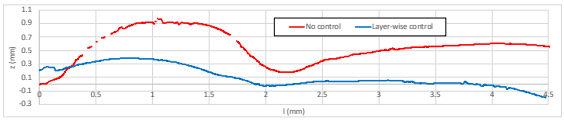

Fig. 13. 3D reconstructions of the produced star specimens a) without (MSE= 6.42 mm^2) and b) with layer-wise control (MSE= 1.19 mm^2). c) Height map from taken perpendicular to the scan direction along the centre.

Fig. *12* and Fig. *13* report the 3D surface reconstructions of the produced specimens. It can be seen that for both of the geometries executed without the control scheme severe swelling occurred around the edges with the smallest scan vectors. It can be observed that the highest swelling regions also correspond to the largest melt pool areas measured by the monitoring system.

The use of the layer-wise control appears to improve the swelling phenomenon significantly. In both geometries, the swelling around the pointy edges could be avoided. The 3D reconstructions showed that the mean square error could be lowered from 8.75 mm^2 to 1.54 mm^2 in the case of the triangle and from 6.42 mm^2 to 1.19 mm^2 for the star shape.

The results show the efficiency of the proposed method. However, several points remain unexplored. The use of a fixed scan direction remains an issue. The method requires further testing on different geometries with acute transition between the scan vector lengths. Moreover, the test geometries were characterized by a constant section along the build direction. The capacity of the strategy on geometries with variable sections should be further assessed. Finally, the response of the method when scanning overhang structures should be further studied.

Conclusions

The present work proposes a layer-wise control scheme for SLM to improve geometrical accuracy, in particular by reducing hot spot formation and swelling phenomenon. The proposed method employs a coaxial melt-pool monitoring system that measures the melt pool area for each layer and corrects the energy density for the next layer by adjusting the duty cycle. The main outcomes of the work can be summarized as the following.

- A layer-wise control strategy can effectively be applied to control geometrical defects due to overheating.
- Heat accumulation is correlated to the scan vector length as melt pool area enlarges around the thin sections.
- Duty cycle of the laser power can be effectively used to reduce the energy density without comprising the scan speed and hence productivity.
- The reaction time for settling to a stable melt pool area was found to be smaller via the use of a correction factor on the duty cycle of the previous layer ($\Delta\delta$) rather than assigning a new duty cycle.

Future works will concentrate on the limitations regarding the use of the layer-wise control scheme. Particular attention will be paid on overheating causes which are not related to scan vector length, such as overhang regions. Evidently the geometrical defects can be linked to metallurgical differences within the built part. The effect of the control strategies on metallurgical properties will also be assessed.

References

[1] M. Brandt, S. J. Sun, M. Leary, S. Feih, J. Elambasseril, and Q. C. Liu, “High-Value SLM Aerospace Components: From Design to Manufacture,” *Adv. Mater. Res.*, vol. 633, no. January, pp. 135–147, 2013.

[2] D. P. Papazoglou, “Additively Manufactured Lattices for Orthopedic Implants and Process Monitoring of Laser-Powder Bed Fusion Using Neural Networks.” 2019.

[3] D. Wang *et al.*, “Research on design optimization and manufacturing of coating pipes for automobile seal based on selective laser melting,” *J. Mater. Process. Technol.*, vol. 273, p. 116227, Nov. 2019.

[4] M. Grasso and B. M. Colosimo, “Process defects and *in situ* monitoring methods in metal powder bed fusion: a review,” *Meas. Sci. Technol.*, vol. 28, no. 4, p. 044005, 2017.

[5] I. Baturynska, O. Semeniuta, and K. Martinsen, “Optimization of Process Parameters for Powder Bed Fusion Additive Manufacturing by Combination of Machine Learning and Finite Element Method: A Conceptual Framework,” *Procedia CIRP*, vol. 67, pp. 227–232, 2018.

[6] L. Scime and J. Beuth, “Using machine learning to identify in-situ melt pool signatures indicative of flaw formation in a laser powder bed fusion additive manufacturing process,” *Addit. Manuf.*, vol. 25, no. November 2018, pp. 151–165, 2019.

[7] J. Fox, F. Lopez, B. Lane, H. Yeung, and S. Grantham, “On the requirements for model-based thermal control of melt pool geometry in laser powder bed fusion additive manufacturing,” *Mater. Sci. Technol. Conf. Exhib. 2016, MS T 2016*, vol. 1, no. November, pp. 133–140, 2016.

[8] L. Mazzoleni, A. G. Demir, L. Caprio, M. Pacher, and B. Previtali, “Real-Time Observation of Melt Pool in Selective Laser Melting: Spatial, Temporal and Wavelength Resolution Criteria,” *IEEE Trans. Instrum. Meas.*, vol. 9456, no. c, pp. 1–1, 2019.

[9] M. Mani, S. Feng, B. Lane, A. Donmez, S. Moylan, and R. Fesperman, “Measurement science needs for real-time control of additive manufacturing powder-bed fusion processes,” *Addit. Manuf. Handb. Prod. Dev. Def. Ind.*, no. February, pp. 629–676, 2017.

[10] J. P. Kruth, P. Mercelis, J. Van Vaerenbergh, and T. Craeghs, “Feedback control of Selective Laser Melting,” *Proc. 3rd Int. Conf. Adv. Res. Virtual Rapid Prototyp. Virtual Rapid Manuf. Adv. Res. Virtual Rapid Prototyp.*, pp. 521–527, 2007.

[11] T. Craeghs, F. Bechmann, S. Berumen, and J. P. Kruth, “Feedback control of Layerwise Laser Melting using optical sensors,” *Phys. Procedia*, vol. 5, no. PART 2, pp. 505–514, 2010.

[12] H. Yeung, B. M. Lane, M. A. Donmez, J. C. Fox, and J. Neira, “Implementation of Advanced Laser Control Strategies for Powder Bed Fusion Systems,” *Procedia Manuf.*, vol. 26, pp. 871–879, 2018.

[13] V. Renken, A. von Freyberg, K. Schünemann, F. Pastors, and A. Fischer, “In-process closed-loop control for stabilising the melt pool temperature in selective laser melting,” *Prog. Addit. Manuf.*, no. 0123456789, 2019.

[14] A. G. Demir, L. Mazzoleni, L. Caprio, M. Pacher, and B. Previtali, “Complementary use of pulsed and continuous wave emission modes to stabilize melt pool geometry in laser powder bed fusion,” *Opt. Laser Technol.*, vol. 113, no. October 2018, pp. 15–26, 2019.

[15] T. Toeppel *et al.*, “3D analysis in laser beam melting based on real-time process monitoring,” *Mater. Sci. Technol. Conf. Exhib. 2016, MS T 2016*, vol. 1, pp. 123–132, 2016.

[16] D. Alberts, D. Schwarze, and G. Witt, “High speed melt pool & laser power monitoring for selective laser melting,” *Proc. Lane 2016*, no. 2015, 2016.

[17] Renishaw, “InfiniAM Spectral - Energy input and melt-pool emissions monitoring for AM systems.” [Online]. Available: https://www.renishaw.com/en/infiniam-spectral--42310. [Accessed: 12-Jun-2019].

[18] EOS, “EOSTATE MeltPool: Real-time process monitoring for EOS M 290.” [Online]. Available: https://www.eos.info/software/monitoring-software/meltpool-monitoring. [Accessed: 12-Jun-2019].

[19] M. Grasso, V. Laguzza, Q. Semeraro, and B. M. Colosimo, “In-Process Monitoring of Selective Laser Melting: Spatial Detection of Defects Via Image Data Analysis,” *J. Manuf. Sci. Eng.*, vol. 139, no. 5, p. 051001, 2016.

[20] A. G. Demir, P. Colombo, and B. Previtali, “From pulsed to continuous wave emission in SLM with contemporary fiber laser sources: effect of temporal and spatial pulse overlap in part quality,” *Int. J. Adv. Manuf. Technol.*, vol. 91, no. 5–8, 2017.

[21] M. Pacher, L. Mazzoleni, L. Caprio, A. G. Demir, and B. Previtali, “Estimation of melt pool size by

complementary use of external illumination and process emission in coaxial monitoring of selective laser melting," *J. Laser Appl.*, vol. 31, no. 2, p. 022305, 2019.

[22] L. Mazzoleni, L. Caprio, M. Pacher, and A. G. Demir, "External Illumination Strategies for Melt Pool Geometry Monitoring in SLM," *JOM*, 2018.

Meet the authors

Ema Vasileska was born in Skopje, North Macedonia in 1993. She has gained a BSc in Mechanical engineering from Ss. Cyril and Methodius University in Skopje in 2015, followed by an MSc in Automation and Control Engineering from the Politecnico di Milano in 2019. Her research interests involve the use of optical monitoring methods and development of control strategies for improving melt pool stability in selective laser melting.

Ali Gökhan Demir was born in Istanbul, Turkey, in 1985. He completed his PhD in Mechanical Engineering at the Politecnico di Milano in collaboration with the University of Cambridge gaining a European PhD title in 2014. He has been an Assistant Professor with the Department of Mechanical Engineering, Politecnico di Milano, since 2015. His current research interests include laser-based manufacturing processes, mainly, additive manufacturing, laser micromachining, and laser welding. Within his research, he gives emphasis to the light-material interaction mechanism in temporal, spatial, and wavelength domains to gather a greater understanding of both existing and new processes.

Bianca Maria Colosimo is Full Professor in the Department of Mechanical Engineering of Politecnico di Milano, where she received her M.S. (cum Laude) in 1996 and her PhD in 2000, both in Industrial Engineering. Her research interest is mainly in the area of Quality Engineering (i.e. statistical process monitoring, control and optimization), with special attention to advanced manufacturing processes, metal additive manufacturing among others. Minor research activities concern process modeling, optimization, metrology and inspection of complex products. She has been leading different research projects, mainly in the area of profile/surface data modeling, monitoring and signal data fusion of manufacturing processes.

Barbara Previtali received her PhD degree in manufacturing and production system from the Politecnico di Milano in 2002. In 2016, she was appointed as Full Professor in the Mechanical Engineering Department, Politecnico di Milano. She leads the SITEC—Laboratory for Laser Applications and PromozioneL@ser with AITeM, which collects Italian laser users in industry and academia. Her current research interests include modeling, optimization and control of laser processes in their application in various fields. On these research subjects, she has authored or coauthored over 100 papers in refereed international journals and international conferences and two international patents.